



Published in final edited form as:

Mol Cancer Res. 2020 April ; 18(4): 599–611. doi:10.1158/1541-7786.MCR-19-0606.

Metabolic Profiling Reveals a Dependency of Human Metastatic Breast Cancer on Mitochondrial Serine and One-Carbon Unit Metabolism

Albert M. Li^{1,2}, Gregory S. Ducker³, Yang Li¹, Jose A. Seoane^{4,5,6}, Yiren Xiao¹, Stavros Melemenidis¹, Yiren Zhou¹, Ling Liu³, Sakari Vanharanta⁷, Edward E. Graves^{1,2}, Erinn B. Rankin^{1,2,6}, Christina Curtis^{2,4,5,6}, Joan Massagué⁸, Joshua D. Rabinowitz³, Craig B. Thompson^{8,*}, Jiangbin Ye^{1,2,6,*}

¹Department of Radiation Oncology, Stanford University School of Medicine. Stanford, CA 94305, US.

²Cancer Biology Program, Stanford University School of Medicine. Stanford, CA 94305, US.

³Lewis-Sigler Institute for Integrative Genomics and Department of Chemistry, Princeton University. Princeton, NJ 08544, US.

⁴Department of Medicine, Stanford University School of Medicine. Stanford, CA 94305, US.

⁵Department of Genetics, Stanford University School of Medicine. Stanford, CA 94305, US.

⁶Stanford Cancer Institute, Stanford University School of Medicine. Stanford, CA 94305, US.

⁷MRC Cancer Unit, University of Cambridge, Hutchison/MRC Research Centre. Cambridge, CB2 0XZ, UK.

⁸Cancer Biology and Genetics Program, Memorial Sloan Kettering Cancer Center. New York, NY 10065, US.

Abstract

Breast cancer is the most common cancer among American women and a major cause of mortality.

To identify metabolic pathways as potential targets to treat metastatic breast cancer, we performed

*Correspondence to: Craig Thompson (thompsonc@mskcc.org), 1275 York Avenue, New York, NY 10065, Tel: 212-639-6561, Jiangbin Ye (yej1@stanford.edu), 269 Campus Drive, Stanford, CA 94305, Tel: 650-724-7459.

Authors' Contributions

Conception and design: A.M. Li, J. Ye, C.B. Thompson, J. Massagué

Development of methodology: A.M. Li, G.S. Ducker, Y. Li, J.A. Seoane, Y. Xiao, S. Melemenidis, E.E. Graves, E. B. Rankin, C. Curtis, J. Ye

Acquisition of data (provided animals, acquired and managed patients, provided facilities, etc.): A.M. Li, G.S. Ducker, Y. Li, Y. Xiao, S. Melemenidis, Y. Zhou, L. Liu, J. Ye

Analysis and interpretation of data (e.g., statistical analysis, biostatistics, computational analysis): A.M. Li, G.S. Ducker, J.A. Seoane, C. Curtis, J. Massagué, J.D. Rabinowitz, C.B. Thompson, J. Ye

Writing, review, and/or revision of the manuscript: A.M. Li, G.S. Ducker, Y. Li, J.A. Seoane, S. Melemenidis, S. Vanharanta, E.E. Graves, E.B. Rankin, C. Curtis, J. Massagué, J.D. Rabinowitz, C.B. Thompson, J. Ye

Study supervision: C.B. Thompson, J. Ye

Other (provided cell lines and plasmids): S. Vanharanta, J. Massagué

Conflict of Interest: C.B.T. is a founder of Agios Pharmaceuticals and a member of its scientific advisory board. He also previously served on the Board of Directors of Merck and Charles River Laboratories. J.D.R. is a co-founder of Raze Therapeutics, advisor to the Barer Institute and L.E.A.F. Pharmaceuticals, and inventor of Princeton University patents regarding 1C metabolism inhibitors. J.M. is scientific advisor and owns stock of Scholar Rock.

metabolomics profiling on breast cancer cell line MDA-MB-231 and its tissue-tropic metastatic subclones. Here, we report that these subclones with increased metastatic potential display an altered metabolic profile compared to the parental population. In particular, the mitochondrial serine and one-carbon (1C) unit pathway is upregulated in metastatic subclones. Mechanistically, the mitochondrial serine and 1C unit pathway drives the faster proliferation of subclones through enhanced *de novo* purine biosynthesis. Inhibition of the first rate-limiting enzyme of the mitochondrial serine and 1C unit pathway, serine hydroxymethyltransferase (SHMT2), potently suppresses proliferation of metastatic subclones in culture and impairs growth of lung metastatic subclones at both primary and metastatic sites in mice. Some human breast cancers exhibit a significant association between the expression of genes in the mitochondrial serine and 1C unit pathway with disease outcome and higher expression of SHMT2 in metastatic tumor tissue compared to primary tumors. In addition to breast cancer, a few other cancer types, such as adrenocortical carcinoma (ACC) and kidney chromophobe cell carcinoma (KICH), also display increased SHMT2 expression during disease progression. Together, these results suggest that mitochondrial serine and 1C unit plays an important role in promoting cancer progression, particularly in late stage cancer.

Keywords

SHMT2; serine; one-carbon unit; cancer metabolism; metastasis

Introduction

The majority of breast cancer patients die from metastatic disease. The process of cancer metastasis involves local invasion into surrounding tissue, dissemination into the bloodstream, extravasation, and eventual colonization of a new tissue. Following a period of dormancy, small numbers of micrometastases eventually proliferate into large macrometastases, or secondary tumors.

Previous studies have illuminated several themes of metabolic reprogramming that occur during metastasis (1–8). However, the majority of these reported site-specific metabolic features of metastatic cancer cells. We reason that breast cancer cells that leave the primary tumor and successfully establish new lesions at distal sites would encounter similar metabolic stresses during metastasis. By performing comparative metabolomics on the MDA-MB-231 human breast cancer cell line and its tissue-tropic metastatic subclones, we uncovered that the catabolism of the non-essential amino acid serine through the mitochondrial one-carbon (1C) unit pathway is an important driver of proliferation in a subset of metastatic breast cancers that closely resembles the molecular features of MDA-MB-231 cells. Emerging evidence shows that the non-essential amino acid serine is essential for cancer cell survival and proliferation. The genomic regions containing PHGDH are amplified in breast cancer and melanoma, diverting 3PG to serine synthesis (9,10). We also reported that PHGDH is upregulated upon amino acid starvation by the transcription factor ATF4 (11). On one hand, serine serves as a precursor for the synthesis of protein, lipids, nucleotides and other amino acids, which are necessary for cell division and growth. On the other hand, serine catabolism through the mitochondrial 1C unit pathway is critical for

maintaining cellular redox control under stress conditions (12,13). In mitochondria, serine catabolism is initiated by serine hydroxymethyltransferase 2 (SHMT2). SHMT2 catalyzes a reversible reaction converting serine to glycine, with concurrent generation of the 1C unit donor methylene-THF, which is further oxidized by downstream enzymes MTHFD2 and MTHFD1L to produce NAD(P)H and formate. Subsequent export of formate from the mitochondria can then be re-assimilated into the cytosolic folate pool to support anabolic reactions. All three mitochondrial serine and 1C unit pathway enzymes (SHMT2, MTHFD2 and MTHFD1L) are upregulated in breast tumor samples compared to normal tissues (13,14). However, due to lack of functional investigations targeting this pathway in *in vitro* and *in vivo* breast cancer models, it remains unclear whether the mitochondrial 1C unit pathway represents a good target for treating metastatic breast cancer.

In this study, we report that enzymes in the mitochondrial serine and 1C unit pathway are even further upregulated specifically in subclones of the aggressive breast cancer cell line MDA-MB-231 that have been selected *in vivo* for the ability to preferentially metastasize to specific organs. We demonstrate that SHMT2 inhibition suppresses proliferation more strongly in these highly metastatic subclones compared to the parental population *in vitro*. Knockdown of SHMT2 also impairs breast cancer growth *in vivo* at both the primary and metastatic sites. In addition, we find that the expression of mitochondrial 1C unit pathway enzymes significantly associates with poor disease outcome in a subset of human breast cancer patients, potentiating its role as a therapeutic target or biomarker in advanced cancer. Finally, SHMT2 expression increases in breast invasive carcinoma, adrenocortical carcinoma, chromophobe renal cell carcinoma and papillary renal cell carcinoma during tumor progression, particularly in late stage tumors, suggesting that inhibitors targeting SHMT2 may hold promise for treating these late stage cancers when other therapeutic options become limited.

Materials and Methods

Cell lines

All of the paired parental and metastatic subclones were generated in Dr. Joan Massagué's laboratory (Memorial Sloan-Kettering Cancer Center) (15–17). Cells were cultured in DMEM/F12 with 10% fetal bovine serum (Sigma) with 1% penicillin/streptomycin. All cells lines were tested every three to six months and found negative for *mycoplasma* (MycoAlert Mycoplasma Detection Kit; Lonza). These cell lines were not authenticated by the authors. All cell lines used in experiments were passaged no more than ten times from time of thawing.

RNAi

Stable 831-BrM, 1833-BoM, and 4175-LM cell lines expressing shRNA against SHMT2, MTHFD2, and c-Myc were generated through infection with lentivirus and 1 µg/mL puromycin selection. shRNA-expressing virus was obtained using a previously published method (13). Pooled populations were tested for on-target knockdown by immunoblot.

Immunoblot

The following antibodies were used: SHMT1, SHMT2 (Sigma), MTHFD2, MTHFD1L, c-Myc, Actin (Cell Signaling Technologies).

RNA Isolation, Reverse Transcription, and Real-Time PCR

Total RNA was isolated from tissue culture plates according to the TRIzol Reagent (Invitrogen) protocol. 3 µg of total RNA was used in the reverse transcription reaction using the SuperScript III (Invitrogen) protocol. Quantitative PCR amplification was performed on the Prism 7900 Sequence Detection System (Applied Biosystems) using Taqman Gene Expression Assays (Applied Biosystems). Gene expression data were normalized to 18S rRNA.

In vivo Tumor Growth Assays

All procedures involving animals and their care were approved by the Institutional Animal Care and Use Committee of Stanford University in accordance with institutional and National Institutes of Health guidelines. For orthotopic growth studies, 4175-LM shNT and 4175-LM shSHMT2 cells (1×10^6 cells in 0.1 mL of PBS, n = 8 per group) were injected into the flanks of NU/J 10-week-old female mice (The Jackson Laboratory). Tumors were measured with calipers over a 50-day time course. Volumes were calculated using the formula $\text{width}^2 \times \text{length} \times 0.5$.

For lung metastasis assays, 4175-LM shNT and 4175-LM shSHMT2 cells (0.2×10^5 cells, n = 8 per group) were injected via tail vein into 6–8 week-old female NOD SCID mice. Mice were imaged weekly using the Xenogen IVIS 200 (PerkinElmer, Waltham, MA). Briefly, mice were injected intraperitoneally with 100 µg/g of D-luciferin (potassium salt; PerkinElmer) on the day of imaging. 8 min later, mice were anesthetized in an anesthesia-induction chamber using a mixture of 3% isoflurane (Fluriso, VetOne) in O₂. Anesthesia was maintained with a mixture of 2% isoflurane in O₂ inside the imaging chamber. Using Living Image (PerkinElmer, Waltham, MA), images were acquired (Exposure time, auto; F stop, 1.2; Binning, medium) from both dorsal and ventral sides of mice and a total photon flux (p/sec/cm²/sr) per animal was calculated by averaging the signal acquired from the dorsal and ventral side. After 4 weeks, surviving mice were sacrificed and lungs snap frozen in liquid N₂ prior to homogenization in TRIzol for RNA extraction.

Metabolite Profiling and Mass Spectrometry

For total metabolite analysis, parental and metastatic cell lines were seeded in 60mm culture dishes in DMEM/F12 supplemented with 10% dialyzed fetal bovine serum. Media was refreshed 2 hours prior to harvesting by washing 3x with PBS before quenching with 800mL of -80 C 80:20 methanol:water. Extracts were spun down, supernatants collected, dried and resuspended in water before LC-MS analysis. Samples were analyzed by reversed-phase ion-pairing chromatography coupled with negative-mode electrospray-ionization high-resolution MS on a stand-alone ThermoElectron Exactive orbitrap mass spectrometer (18). Peak picking and quantification were conducted using MAVEN analysis software. Heatmap was generated in R. Multiple testing correction and q-value generation were performed in PRISM software (GraphPad).

For [2,3,3-²H]serine labeling experiments, parental and metastatic cells were cultured in RPMI medium lacking glucose, serine, and glycine (TEKnova) supplemented with 2 g/L glucose and 0.03 g/L [2,3,3-²H]serine (Cambridge Isotope Laboratories) for up to 24 hours before harvesting. Cells were washed twice with ice-cold PBS prior to extraction with 400 µL of 80:20 acetonitrile:water over ice for 15 min. Cells were scraped off plates to be collected with supernatants, sonicated for 30s, then spun down at 1.5×10^4 RPM for 10 min. 200 µL of supernatant was taken out for LC-MS/MS analysis immediately.

Quantitative LC-ESI-MS/MS analysis of [2,3,3-²H]serine-labeled cell extracts was performed using an Agilent 1290 UHPLC system equipped with an Agilent 6545 Q-TOF mass spectrometer (Santa Clara, CA, US). A hydrophilic interaction chromatography method (HILIC) with an BEH amide column (100 × 2.1 mm i.d., 1.7 µm; Waters) was used for compound separation at 35 °C with a flow rate of 0.3ml/min. The mobile phase A consisted of 25 mM ammonium acetate and 25mM ammonium hydroxide in water and mobile phase B was acetonitrile. The gradient elution was 0–1 min, 85 % B; 1–12 min, 85 % B → 65 % B; 12– 12.2 min, 65 % B-40%B; 12.2–15 min, 40%B. After the gradient, the column was re-equilibrated at 85%B for 5min. The overall runtime was 20 min and the injection volume was 5 µL. Agilent Q-TOF was operated in negative mode and the relevant parameters were as listed: ion spray voltage, 3500 V; nozzle voltage, 1000 V; fragmentor voltage, 125 V; drying gas flow, 11 L/min; capillary temperature, 325 °C, drying gas temperature, 350 °C; and nebulizer pressure, 40 psi. A full scan range was set at 50 to 1600 (m/z). The reference masses were 119.0363 and 980.0164. The acquisition rate was 2 spectra/s. Isotopologues extraction was performed in Agilent Profinder B.08.00 (Agilent Technologies). Retention time (RT) of each metabolite was determined by authentic standards (Supplementary Table S1). The mass tolerance was set to +/-15 ppm and RT tolerance was +/- 0.2 min. Natural isotope abundance was corrected using Agilent Profinder software (Agilent Technologies).

Cell Line Classification

Cell line expression and copy number data were downloaded from the COSMIC cell line dataset (https://cancer.sanger.ac.uk/cell_lines), and all cell lines were classified using different cell line classifiers, including PAM50 and scmod2 using the package geneFu from Bioconductor; and iC10 using package iC10 (19–22). The MDA-MB-231 parental and metastatic subclones were classified as Basal (posterior probability of 0.516), ER-Her2- (posterior probability of 0.997), IC4 (posterior probability of 0.999).

Outcome Analysis

METABRIC clinical and expression data was downloaded from EGA (EGAS00000000083) (21). Outcome analysis was performed in IC4 samples only (N=342) in order to mimic the phenotype of the MDA-MB-231 breast cancer cell line. Survival analysis was performed over disease specific survival (DSS) censored to 20 years. Gene high/low categorization was performed using the maxstat algorithm, which determines the optimal threshold for separating high and low expression (from the surv cutpoint function of package survminer). Cox Proportional Hazard multivariate models use continuous expression adjusted by age, grade, size, number of lymph nodes, ER, PR and Her2 status. Kaplan-Meier plots were

generated using the package `survcomp`, and Cox Proportional Hazards were generated using the package `rms`.

Immunohistochemical Staining and Quantification for SHMT2

Human primary breast cancer tissue and paired lymph node metastases were obtained from Biomax.us. Tumors were graded by Biomax.us pathologists according to the Nottingham grading system with respect to degree of glandular duct formation, nuclear pleomorphism, and nuclear fission counting. Each feature was scored from 1–3, and the total score was used to determine the following grades: Grade 1 (total score 3–5; low grade or well differentiated), Grade 2 (total score 6–7; intermediate grade or moderately differentiated), Grade 3 (total score 8–9; high grade or poorly differentiated). Standard immunohistochemical methods were performed as previously described (23). The primary anti-human SHMT2 antibody (Sigma) was used at a concentration of 1:3000. Images were acquired on a Leica DMI8 system (Leica Microsystems) and quantified for positive SHMT2 signal intensity by ImageJ software.

SHMT2 Expression Analysis by Individual Cancer Stage

SHMT2 expression data across every annotated TCGA cancer data set was queried and downloaded from the UALCAN database (<http://ualcan.path.uab.edu/index.html>) (24).

Statistical Analyses

All statistical tests were performed using the paired or unpaired Student's t test by PRISM software. Values with a p value of < 0.05 were considered significant.

Results

Metastatic breast cancer cells exhibit altered metabolic profiles

To identify common metabolic pathways reprogrammed in metastatic breast cancer cells during cancer progression, we performed metabolomic profiling of the human triple negative breast cancer cell line MDA-MB-231 and its metastatic subpopulations (Fig. 1A and B). This cell line was derived from the pleural effusion of a patient with widespread metastatic disease years after primary tumor removal (25), and the subclones of this cell line with higher metastasis rate and preference to the bone, lung, or brain were previously isolated by *in vivo* selection (15–17) (831-BrM: brain metastasis. 1833-BoM: bone metastasis. 4175-LM: lung metastasis).

At the time of initial metabolomics comparison, the lung metastatic subclone 4175-LM did not recover well in culture, so we profiled the 831-BrM and 1833-BoM metastatic subclones along with the parental population. We observed multiple metabolites involved in a plethora of metabolic pathways that were differentially enriched or depleted in the metastatic 831-BrM and 1833-BoM subclones compared to the parental population of MDA-MB-231 (231-Parental) cells (Fig. 1B). Following correction for false discovery rate, the levels of twenty-four metabolites were significantly altered in both 831-BrM and 1833-BoM cells compared to 231-Parental cells (Supplementary Table S2). Metabolites significantly enriched in metastatic subclones included the glycolytic intermediate dihydroxyacetone-phosphate

(which is reversibly isomerized to glyceraldehyde-3-phosphate), the tricarboxylic acid (TCA) cycle intermediate succinate, amino acids such as proline and asparagine, and the pentose-phosphate pathway product 5-phosphoribosyl-1-pyrophosphate. These observations are consistent with prior observations of perturbations in lower glycolysis and the TCA cycle observed in other cell line models (notably murine 4T1 cells), suggesting common metabolic developments during metastasis of breast cancers in both mice and humans (1–3,5,6). Additionally, enrichment of asparagine has been reported to promote metastatic cancer cell phenotypes by epithelial-to-mesenchymal transition (8). Nonetheless, the most significantly depleted class of metabolites in 831-BrM and 1833-BoM cells compared to 231-Parental cells were free purine nucleotides, suggesting alterations in purine metabolism in metastatic cells (Fig. 1B).

c-Myc is important for breast cancer cell proliferation

We wondered whether reduced levels of purines reflected decreased synthesis or higher consumption in the metastatic subclones. Because it was previously reported that the oncogenic transcription factor c-Myc induces the expression of nucleotide biosynthesis genes and that c-Myc amplification and overexpression is a common event in triple-negative breast cancer (26–28), we wondered if the relative differences in purine abundance could be explained by altered c-Myc protein levels in our cell line system. Indeed, 831-BrM, 1833-BoM, and 4175-LM cells overexpressed c-Myc compared to 231-Parental cells (Fig. 2A). Since sufficiency of free nucleotides can act as an important checkpoint for cell division (29), we then compared the proliferation rates of parental and metastatic subclones. Accordingly, 831-BrM, 1833-BoM, and 4175-LM cells proliferated faster than 231-Parental cells *in vitro* (Fig. 2B), suggesting that the higher consumption rate is the cause of lower purine levels in the metastatic subclones.

Because the role of c-Myc in metastasis is still unclear, with evidence suggesting it plays both pro-metastatic and anti-metastatic functions in breast cancer depending on the genetic context (30,31), we tested the sensitivity of parental and metastatic subclones to c-Myc inhibition. Small hairpin RNA (shRNA)-mediated knockdown of c-Myc reduced cell proliferation in all four cell lines, although the degree of inhibition was stronger in 831-BrM and 1833-BoM cells (Fig. 2C, Supplementary Fig. S1). Parental cells expressing a non-targeting shRNA showed elevated c-Myc expression, possibly due to puromycin selection. These data suggest that c-Myc is an important mediator of cell proliferation, and c-Myc overexpression provided a proliferative advantage at least in brain and bone-metastatic subclones.

Identification of serine and one-carbon unit pathway elevation in metastatic subclones

The products of several metabolic pathways feed into nucleotide synthesis, including ribulose-5-phosphate from the pentose phosphate pathway, and one-carbon (1C) units and glycine from the serine and 1C unit pathway. It is also known that c-Myc can promote the expression of serine and glycine metabolism genes in cancer cells (32,33). We performed expression analyses of the metastatic subclones and found elevated levels of the key mitochondrial enzymes serine hydroxymethyltransferase 2 (SHMT2), methylenetetrahydrofolate dehydrogenase 2 (MTHFD2), and methylenetetrahydrofolate

dehydrogenase 1-like (MTHFD1L), in contrast to the downregulated expression of the cytosolic isoenzyme serine hydroxymethyltransferase 1 (SHMT1) (Fig. 3A–C). Consistent with previous reports in other cell types, knockdown of c-Myc in parental and metastatic breast cancer subclones diminished MTHFD2 and MTHFD1L protein expression, suggesting these enzymes are c-Myc-regulated (Supplementary Fig. S1). SHMT2 expression did not reduce upon c-Myc knockdown, suggesting that SHMT2 expression was regulated by other transcription factors. To determine whether c-Myc and mitochondrial 1C unit pathway enzyme overexpression was a common co-occurrence in other cancer metastasis models, we checked protein expression levels in the parental and metastatic subpopulations of other human cell line systems derived from lung adenocarcinoma or ER⁺ breast carcinoma patients (34,35). There was a clear correlation of SHMT2, MTHFD2, and MTHFD1L expression with c-Myc expression among all the cell lines tested. The brain metastatic subclones of lung adenocarcinoma cell lines PC9 and H2030 had increased MTHFD2 expression, though we could not find another system that also displayed overexpression of c-Myc and all the three mitochondrial 1C unit pathway enzymes in metastatic subclones relative to their corresponding parental cells (Supplementary Fig. S2). Taken together with the observations of higher serine and glycine levels in 831-BrM and 1833-BoM cells compared to 231-Parental cells (Fig. 1B), these data suggest that the role of c-Myc in regulating mitochondrial serine and 1C unit metabolism in metastatic cancer may be tissue-specific.

Metastatic subclones display increased mitochondrial serine and one-carbon unit pathway activity

We next asked if higher expression of mitochondrial serine and 1C unit pathway enzymes might indeed reflect higher pathway activity. Serine can be catabolized in both the mitochondrial and cytosolic branch of the 1C unit pathway. Since cancer cells predominately express the mitochondrial serine catabolic enzymes over the cytosolic enzymes, serine is generally catabolized in the mitochondria in cancer cells (13,14,36). Serine hydroxymethyltransferase 2 (SHMT2) initiates this reaction by converting serine to glycine while donating a carbon group to tetrahydrofolate (THF) to generate methylene-THF. Subsequent oxidation of methylene-THF by MTHFD2 and MTHFD1L generates NAD(P)H and formate. Formate can cross the mitochondrial membrane to provide 1C units for anabolic reactions such as nucleotide synthesis (37).

We hypothesized that the reason metastatic cells upregulate the serine and 1C unit pathway is to enhance nucleotide synthesis to fuel cell proliferation. Indeed, most cancer cells have been reported to utilize serine as the predominant source of 1C units for biosynthesis (38). We performed [2,3,3-²H]serine tracing to examine 1C unit pathway flux to glycine and purine nucleotides. In cells grown in media containing [2,3,3-²H]serine, the cytosolic pathway generates methylene-THF (me-THF) mass heavy by 2 (M+2) and 10-formyl-THF mass heavy by 1 (M+1), while 10-formyl-THF derived from mitochondrial formate exchange to the cytosol is strictly M+1. [2,3,3-²H]serine labeling onto the metabolites glycine and purine nucleotide triphosphates produced from the mitochondrial pathway thereby produces glycine M+1 and purines either M+1 or M+2 (Fig. 3D). Time course experiments were performed in 4175-LM cells to determine the optimal steady state labeling

conditions for glycine and ATP from serine: 2 hours and 24 hours respectively (Supplementary Fig. S3). We observed higher SHMT flux in metastatic subclones, as the relative abundance of M+1 glycine was approximately 1.5-fold higher in 4175-LM cells compared to 231-Parental cells, indicating that higher purine turnover in metastatic cells was fueled by higher SHMT flux (Fig. 3E). Importantly, while robust fractions of ATP and GTP were labeled in parental cells, the metastatic subclones displayed even higher labeling fractions from serine (Fig. 3F). These results demonstrate that upregulation of serine catabolism through the mitochondrial 1C unit pathway promotes *de novo* purine synthesis in metastatic breast cancer cells.

Serine catabolism is necessary for metastatic cancer cell proliferation *in vitro*

To address the extent to which mitochondrial serine catabolism is necessary for cell proliferation, 231-Parental, 831-BrM, 1833-BoM, and 4175-LM cells were infected with lentivirus expressing shRNAs against SHMT2 (shSHMT2) or a nontargeting control (shNT). Intriguingly, knockdown of SHMT2 protein expression with two different shRNAs drastically suppressed proliferation of the metastatic subclones significantly, with a reduced effect in 231-Parental cells (Fig. 4A and B). In contrast, knockdown of the downstream enzyme of the mitochondrial serine and 1C unit pathway, MTHFD2, suppressed proliferation to a lesser extent (Supplementary Fig. S4A and B). To evaluate the therapeutic potential of targeting 1C unit metabolism to block metastatic growth, we treated cells with a small-molecule inhibitor of SHMT called SHIN1 (39). *In vitro*, metastatic subclones were sensitive to SHIN1 with an EC50 in the 100–500 nM range (Supplementary Fig. S5). There was no obvious enhancement of SHIN1 sensitivity in 831-BrM, 1833-BoM, and 4175-LM cells compared to 231-Parental cells, possibly because SHIN1 inhibits both SHMT2 and SHMT1 (Fig. 4C). Importantly, inhibition of cell proliferation in the presence of SHIN1 could be rescued by the supplementation of formate (2 mM), a source of cellular 1C units (Fig. 4C). These results indicate that the major role of elevated mitochondrial serine catabolism is to generate 1C units for cytosolic purine biosynthesis in the metastatic subclones. Thus, targeting SHMT activity may be a promising way to restrict nucleotide availability to block metastatic breast cancer cell proliferation.

SHMT2 knockdown impairs primary and metastatic growth *in vivo*

We then interrogated the effect of reducing mitochondrial 1C unit pathway activity in two different models of cancer growth *in vivo*. 4175-LM cells were chosen due to the relative ease of monitoring, measuring, and collecting tissue from lung metastasis compared to brain and bone metastasis. For the first model, we monitored breast cancer growth at the primary tumor site. SHMT2 knockdown significantly impaired the growth of 4175-LM cells in the mammary fat pads of immunodeficient mice (Fig. 4D, Supplementary Fig. S6). For the second model, we induced breast cancer metastasis to the lung by intravenous tail vein injection. Because 4175-LM cells express firefly luciferase (16), we tracked tumor growth in the lung by bioluminescence imaging (BLI). Both BLI and quantification of human GAPDH (hGAPDH) expression from resected mouse lungs revealed a roughly two-fold reduction of lung tumor burden in mice injected with shSHMT2 cells compared to shNT cells (Fig. 4E and F, Supplementary Fig. S7A). While on average, shSHMT2 tumors had reduced human SHMT2 (hSHMT2) expression compared to shNT tumors, some shSHMT2 tumors appeared

to have reacquired hSHMT2 expression (Supplementary Fig. S7B and C). These data suggest that SHMT2 is necessary for metastatic growth *in vivo*.

Mitochondrial serine and 1C unit pathway genes are associated with more aggressive metastatic disease in some human breast cancer patients

To further explore the relevancy of mitochondrial one-carbon unit metabolism in human breast cancer metastasis, we examined the expression of SHMT1, SHMT2, MTHFD2, and MTHFD1L in the METABRIC dataset of human breast cancer patients (21). We retrospectively inferred metastatic recurrence in patients by examining the frequency of disease-specific survival (DSS) up to 20 years. Patients were separated into two groups based on the maxstat algorithm (see Materials and Methods). Patients with high SHMT2 expression were significantly more likely to succumb to metastatic recurrent disease, while patients with high expression of the cytosolic isozyme SHMT1 were significantly protected from metastatic relapse (Fig. 5A, Supplementary Fig. S8). Using three different breast cancer subtype clustering analyses based on gene expression (PAM50, IC10, SCMOD2), we classified the MDA-MB-231 cell line as basal, IC4 (copy number flat), and ER⁻Her2⁻ (20,21). We have previously described IC4 as consisting of a mixture of ER⁻ tumors with lymphocytic infiltration and ER⁺ tumors with abundant stroma. Accordingly, further analysis of the IC4 patient subgroup following adjustment for covariates of age, grade, size, number of lymph nodes, ER, PR and Her2 status revealed a significant association of MTHFD1, MTHFD1L, MTHFD2, and SHMT2 expression with worse survival and SHMT1 expression with better survival (Fig. 5B). Finally, we stained a tissue microarray panel of human breast invasive ductal carcinoma and matched lymph node metastases and found significantly higher expression of SHMT2 in metastatic cancer cells comparing to the primary tumors (Fig. 5C and D). Together, these data suggest that SHMT2 and other mitochondrial 1C unit pathway enzymes may be used as prognostic markers that indicate worse patient outcome, while cytosolic SHMT1 expression may indicate better survival rate in the IC4 patient subgroup.

Relevance of SHMT2 expression in the progression and aggressiveness of other cancer types

To evaluate the contribution of mitochondrial 1C unit metabolism to the progression of other cancer types, we queried SHMT2 expression in TCGA datasets through the UALCAN portal (24). In addition to breast invasive carcinoma (BRCA), we identified adrenocortical carcinoma (ACC), head and neck squamous cell carcinoma (HNSC), kidney chromophobe cell carcinoma (KICH), and kidney renal papillary cell carcinoma (KIRP) as cancer types in which SHMT2 expression progressively increased as a function of stage (Fig. 6). Notably, gain of SHMT2 expression in BRCA and HNSC tended to occur early on in cancer progression, whereas in KICH, SHMT2 upregulation may occur only during the very late stage. A few cancer types such as mesothelioma (MESO) and ovarian serous cystadenocarcinoma (OV) showed the opposite trend: a progressive loss of SHMT2 expression with increasing cancer stage (Supplementary Fig. 9). Collectively, these data present the possibility that there exist additional cancer types in which mitochondrial 1C unit metabolism promotes progression and aggressiveness.

Discussion

For breast cancer, common metastatic sites include the brain, bone, liver, and lung. At the cellular level, the original heterogeneous population of cancer cells from the primary tumor undergo a selection process whereby those clones with alterations (carrying both genetic lesions and epigenetic modifications) favoring fitness and plasticity are enriched. These adaptations, in turn, equip cells with the ability to withstand standard treatments such as chemotherapy and radiation therapy, ultimately leading to cancer progression and metastatic recurrence (40). While many previous studies have elucidated a role for molecular processes such as epithelial to mesenchymal transition and invasion and migration of cancer cells, our understanding of how metabolic pathway alterations shape metastatic growth is still limited. It is important to note that the MDA-MB-231 cells we studied were isolated from a pleural population that already metastasizes well *in vivo*. Our metabolomics profiling of the even more highly metastatic triple-negative breast cancer subclones suggested alterations in both glycolysis and the TCA cycle during the late stages of cancer progression, consistent with findings from other groups of heightened mitochondrial metabolism in metastatic cells (2,3,5,6). We further discovered elevated catabolism of serine in the mitochondria of our metastatic subclones. A previous study in isogenic murine 4T1 breast cancer cell lines found that transformed cells showed higher levels of nucleotides than nontransformed cells, and that “more metastatic” lines had even more nucleotides than “less metastatic” ones (1). In contrast, we found lower levels of free purines in metastatic variants of human MDA-MB-231 cell lines compared to the parental population (Fig. 1B). This discrepancy may be attributed to different oncogenic contexts in 4T1 cells versus MDA-MB-231 cells or inherent differences in purine metabolism between murine and human cells. Due to the difficulty of obtaining pure metastatic tumor tissue from *in vivo* studies, the metabolomic analysis were performed using established cell lines *in vitro*. Microenvironmental factors from metastatic niche, such as hypoxia and nutrient starvation, also regulate cancer cell metabolism. Since mitochondrial IC unit metabolism can utilize both NAD^+ and NADP^+ , cancer cells with upregulation of mitochondrial IC unit metabolism may gain metabolic flexibility to sustain proliferation under stress conditions. When cells engage active respiration, the mitochondrial IC unit pathway can utilize NAD^+ to generate IC units; under hypoxia or starvation conditions, when the NAD^+/NADH ratio decreases, elevated mitochondrial ROS leads to an increased $\text{NADP}^+/\text{NADPH}$ ratio, which can also drive the IC unit pathway and purine synthesis. Further investigations comparing the metabolic profile changes under these stress conditions may provide more insight into potential links between metabolic stresses and the evolution of metastatic cancer cells.

The role of serine in cancer growth has drawn increasing interest over the years ever since the identification of PHGDH amplifications in melanoma and breast cancer (9,10). A variety of mechanisms have been proposed to explain why increased serine synthesis and serine catabolism could promote tumorigenesis, including rerouting glucose carbon flux, maintenance of compartment-specific $\text{NAD(P)}^+/\text{NAD(P)H}$ ratios, and the control of metabolites such as acetyl-coA, α -ketoglutarate, or 2-hydroxyglutarate (12,41,42). Moreover, a previous study had implicated SHMT2 and a neutral amino acid importer of serine and glycine (ASCT2) as prognostic biomarkers for breast cancer (43). Our study is

the first to directly evaluate the therapeutic potential of targeting SHMT2 in metastatic breast cancer using both genetic and pharmaceutical approaches. Intriguingly, genetic knockdown of SHMT2 strongly inhibited the proliferation of metastatic cells, while treatment with a dual SHMT1/SHMT2 inhibitor suppressed proliferation of both parental and metastatic subclones. This discrepancy may be explained by prior observations that while MDA-MB-231 cells preferentially utilize the mitochondrial pathway for 1C unit production, inhibition of individual mitochondrial enzymes can lead to a switch to the cytosolic pathway (36). We thus speculate that 231-Parental cells may be more adept at switching to cytosolic serine catabolism, and for reasons still unclear, the metastatic subclones are less flexible. Consistent with observations in colon cancer xenografts (36), SHMT2 knockdown in the lung metastatic subclone slowed, but not completely suppressed, tumor growth in the mammary fat pad and lung. In addition, we found that in the IC4 subset of human breast cancer patients, the expression of mitochondrial one-carbon unit enzymes is positively associated with more aggressive disease. Thus, interrogating the expression status of mitochondrial one-carbon unit enzymes through transcriptional or proteomic methods holds prognostic value in the metastatic setting, and warrants the need for further development of drugs that selectively inhibit serine catabolism for treating the metastasis of triple-negative breast cancer.

What causes the upregulation of mitochondrial serine catabolic flux in highly metastatic cancer cells? We provide evidence that a crucial oncogenic event promotes the ability of metastatic breast cancer subclones to catabolize serine faster than parental cells: c-Myc activation. c-Myc overexpression is known to be associated with up to 40% of breast cancers, with hyperactive c-Myc enriched particularly in the basal-like subtype (27,44). These observations are consistent with our findings of the MDA-MB-231 cell line as basal-like and its metastatic subclones expressing even higher levels of c-Myc than the parental population (Fig. 2A). We found that c-Myc was required for the maintenance of the mitochondrial serine and 1C unit pathway genes MTHFD2 and MTHFD1L, consistent with previous reports that c-Myc supports serine/glycine metabolism at the transcriptional level in other cell types (32,33). These results suggest a model for breast cancer metastasis in which a small fraction of c-Myc^{high} expressing cells from the primary tumor acquire the ability to upregulate serine catabolism to fuel growth in metastatic tissue sites. Alternatively, high c-Myc expression and the linked ability to upregulate serine catabolism may be intrinsic properties of stem-like metastasis-initiating cells that are enriched in breast cancer cell populations selected for high metastatic activity in mice. As one of the key oncogenic transcription factors, there is increasing evidence that c-Myc plays multiple roles during the metastatic process. c-Myc knockdown reduces invasion and migration of MDA-MB-231 cells (30). Moreover, a recent study corroborated our findings of elevated c-Myc levels in brain-metastatic derivatives of human breast cancer cells and demonstrated its necessity for the invasive growth of brain metastases (45). Our study highlights the role of c-Myc in enhancing 1C unit pathway activity and proliferation, which is also important for metastatic growth. Since SHMT2 expression was not reduced by c-Myc shRNA, it is likely that other tumor-promoting factors, such as ATF4 and NRF2, also play important roles in late stage cancer progression by modulating 1C unit metabolism. Intriguingly, a recent report showed that TGF- β signaling induces the expression of SHMT2 (46). Given the critical role of TGF-

β in promoting metastasis (47,48), it may be interesting to further investigate whether serine and 1C unit pathway metabolic reprogramming is controlled by TGF- β signaling in metastatic subpopulations of human breast cancer cells.

Supplementary Material

Refer to Web version on PubMed Central for supplementary material.

Acknowledgements

We thank J.T. Eggold for assistance with Leica microscopy; T. Doyle for assistance with bioluminescence imaging; D. Luong for technical assistance; and members of the E.B.R. and J.Y. labs for general assistance and fruitful discussions.

Financial Support: This work was supported by a NIH T32 Training Grant (CA009302-40) to A.M.L., and a NIH R00 Grant (CA184239) and a Mary Kay Foundation Innovative Cancer Research Award (017-37) to J.Y. G.S.D. was supported by NCI K99 CA215307.

References:

1. Lu X, Bennet B, Mu E, Rabinowitz J, Kang Y. Metabolomic changes accompanying transformation and acquisition of metastatic potential in a syngeneic mouse mammary tumor model. *J Biol Chem*. 2010;285:9317–21. [PubMed: 20139083]
2. Porporato PE, Payen VL, Pérez-Escuredo J, De Saedeleer CJ, Danhier P, Copetti T, et al. A mitochondrial switch promotes tumor metastasis. *Cell Rep*. 2014;8:754–66. [PubMed: 25066121]
3. LeBleu VS, O'Connell JT, Gonzalez Herrera KN, Wikman H, Pantel K, Haigis MC, et al. PGC-1 α mediates mitochondrial biogenesis and oxidative phosphorylation in cancer cells to promote metastasis. *Nat Cell Biol*. 2014;16:992–1003. [PubMed: 25241037]
4. Piskounova E, Agathocleous M, Murphy MM, Hu Z, Huddleston SE, Zhao Z, et al. Oxidative stress inhibits distant metastasis by human melanoma cells. *Nature*. 2015;527:186–191. [PubMed: 26466563]
5. Dupuy F, Tabariès S, Andrzejewski S, Dong Z, Blagih J, Annis MG, et al. PDK1-dependent metabolic reprogramming dictates metastatic potential in breast cancer. *Cell Metab*. 2015;22:577–589. [PubMed: 26365179]
6. Christen S, Lorendeau D, Schmieder R, Broekaert D, Metzger K, Veys K, et al. Breast cancer-derived lung metastases show increased pyruvate carboxylase-dependent anaplerosis. *Cell Rep*. 2016;17:837–848. [PubMed: 27732858]
7. Elia I, Broekaert D, Christen S, Boon R, Radaelli E, Orth MF, et al. Proline metabolism supports metastasis formation and could be inhibited to selectively target metastasizing cancer cells. *Nat Commun*. 2017;8:1–11. [PubMed: 28232747]
8. Knott SRV, Wagenblast E, Khan S, Kim SY, Soto M, Wagner M, et al. Asparagine bioavailability governs metastasis in a model of breast cancer. *Nature*. 2018;554:378–381. [PubMed: 29414946]
9. Locasale JW, Grassian AR, Melman T, Lyssiotis CA, Mattaini KR, Bass AJ, et al. Phosphoglycerate dehydrogenase diverts glycolytic flux and contributes to oncogenesis. *Nat Genet*. 2011;43:869–74. [PubMed: 21804546]
10. Possemato R, Marks KM, Shaul YD, Pacold ME, Kim D, Birsoy K, et al. Functional genomics reveal that the serine synthesis pathway is essential in breast cancer. *Nature*. 2011;476:346–50. [PubMed: 21760589]
11. Ye J, Mancuso A, Tong X, Ward PS, Fan J, Rabinowitz JD, et al. Pyruvate kinase M2 promotes de novo serine synthesis to sustain mTORC1 activity and cell proliferation. *Proc Natl Acad Sci*. 2012;109:6904–9. [PubMed: 22509023]
12. Fan J, Ye J, Kamphorst JJ, Shlomi T, Thompson CB, Rabinowitz JD. Quantitative flux analysis reveals folate-dependent NADPH production. *Nature*. 2014;510:298–302. [PubMed: 24805240]

13. Ye J, Fan J, Venneti S, Wan YW, Pawel BR, Zhang J, et al. Serine catabolism regulates mitochondrial redox control during hypoxia. *Cancer Discov.* 2014;4:1406–17. [PubMed: 25186948]
14. Nilsson R, Jain M, Madhusudhan N, Sheppard NG, Strittmatter L, Kampf C, et al. Metabolic enzyme expression highlights a key role for MTHFD2 and the mitochondrial folate pathway in cancer. *Nat Commun.* 2014;5:3128. [PubMed: 24451681]
15. Kang Y, Siegel PM, Shu W, Drobnjak M, Kakonen SM, Córdón-Cardo C, et al. A multigenic program mediating breast cancer metastasis to bone. *Cancer Cell.* 2003;3:537–49. [PubMed: 12842083]
16. Minn AJ, Gupta GP, Siegel PM, Bos PD, Shu W, Giri DD, et al. Genes that mediate breast cancer metastasis to lung. *Nature.* 2005;436:518–24. [PubMed: 16049480]
17. Bos PD, Zhang XH-F, Nadal C, Shu W, Gomis RR, Nguyen DX, et al. Genes that mediate breast cancer metastasis to the brain. *Nature.* 2009;459:1005–9. [PubMed: 19421193]
18. Lu W, Clasquin MF, Melamud E, Amador-Noguez D, Caudy AA, Rabinowitz JD. Metabolomic analysis via reversed-phase ion-pairing liquid chromatography coupled to a stand alone orbitrap mass spectrometer. *Anal Chem.* 2010;82:3212–21. [PubMed: 20349993]
19. Wirapati P, Sotiriou C, Kunkel S, Farmer P, Pradervand S, Haibe-Kains B, et al. Meta-analysis of gene expression profiles in breast cancer: toward a unified understanding of breast cancer subtyping and prognosis signatures. *Breast Cancer Res.* 2008;10:R65. [PubMed: 18662380]
20. Parker JS, Mullins M, Cheang MCU, Leung S, Voduc D, Vickery T, et al. Supervised risk predictor of breast cancer based on intrinsic subtypes. *J Clin Oncol.* 2009;27:1160–7. [PubMed: 19204204]
21. Curtis C, Shah SP, Chin SF, Turashvili G, Rueda OM, Dunning MJ, et al. The genomic and transcriptomic architecture of 2,000 breast tumours reveals novel subgroups. *Nature.* 2012;486:346–352. [PubMed: 22522925]
22. Ali HR, Rueda OM, Chin S-F, Curtis C, Dunning MJ, Aparicio SAJR, et al. Genome-driven integrated classification of breast cancer validated in over 7,500 samples. *Genome Biol.* 2014;15:431. [PubMed: 25164602]
23. Rankin EB, Fuh KC, Castellini L, Viswanathan K, Finger EC, Diep AN, et al. Direct regulation of GAS6/AXL signaling by HIF promotes renal metastasis through SRC and MET. *Proc Natl Acad Sci U A.* 2014;111:13373–13378.
24. Chandrashekar DS, Bachel B, Balasubramanya SAH, Creighton CJ, Ponce-Rodriguez I, Chakravarthi BVS, et al. UALCAN: A Portal for Facilitating Tumor Subgroup Gene Expression and Survival Analyses. *Neoplasia.* 2017;19:649–58. [PubMed: 28732212]
25. Cailleau R, Olivé M, Cruciger QVJ. Long-term human breast carcinoma cell lines of metastatic origin: Preliminary characterization. *In Vitro.* 1978;14:911–5. [PubMed: 730202]
26. Liu Y-C, Li F, Handler J, Huang CRL, Xiang Y, Neretti N, et al. Global regulation of nucleotide biosynthetic genes by c-Myc. *PLoS ONE.* 2008;3:e2722. [PubMed: 18628958]
27. Horiuchi D, Kusdra L, Huskey NE, Chandriani S, Lenburg ME, Gonzalez-Angulo AM, et al. MYC pathway activation in triple-negative breast cancer is synthetic lethal with CDK inhibition. *J Exp Med.* 2012;209:679–96. [PubMed: 22430491]
28. Muhar M, Ebert A, Neumann T, Umkehrer C, Jude J, Wieshofer C, et al. SLAM-seq defines direct gene-regulatory functions of the BRD4-MYC axis. *Science.* 2018;360:800–5. [PubMed: 29622725]
29. Ewald B, Sampath D, Plunkett W. Nucleoside analogs: molecular mechanisms signaling cell death. *Oncogene.* 2008;27:6522–37. [PubMed: 18955977]
30. Wolfer A, Wittner BS, Irimia D, Flavin RJ, Lupien M, Gunawardane RN, et al. MYC regulation of a “poor-prognosis” metastatic cancer cell state. *Proc Natl Acad Sci.* 2010;107:3698–703. [PubMed: 20133671]
31. Liu H, Radisky DC, Yang D, Xu R, Radisky ES, Bissell MJ, et al. MYC suppresses cancer metastasis by direct transcriptional silencing of α v and β 3 integrin subunits. *Nat Cell Biol.* 2012;14:567–74. [PubMed: 22581054]
32. Nikiforov MA, Chandriani S, O’Connell B, Petrenko O, Kottenko I, Beavis A, et al. A functional screen for Myc-responsive genes reveals serine hydroxymethyltransferase, a major source of the one-carbon unit for cell metabolism. *Mol Cell Biol.* 2002;22:5793–800. [PubMed: 12138190]

33. Sun L, Song L, Wan Q, Wu G, Li X, Wang Y, et al. cMyc-mediated activation of serine biosynthesis pathway is critical for cancer progression under nutrient deprivation conditions. *Cell Res.* 2015;25:429–444. [PubMed: 25793315]
34. Valiente M, Obenauf AC, Jin X, Chen Q, Zhang XH-F, Lee DJ, et al. Serpins promote cancer cell survival and vascular co-option in brain metastasis. *Cell.* 2014;156:1002–16. [PubMed: 24581498]
35. Malladi S, Macalinao DG, Jin X, He L, Basnet H, Zou Y, et al. Metastatic latency and immune evasion through autocrine inhibition of WNT. *Cell.* 2016;165:45–60. [PubMed: 27015306]
36. Ducker GS, Chen L, Morscher RJ, Teng X, Kang Y, Rabinowitz JD, et al. Reversal of cytosolic one-carbon flux compensates for loss of the mitochondrial folate pathway. *Cell Metab.* 2016;23:1140–1153. [PubMed: 27211901]
37. Ducker GS, Rabinowitz JD. One-carbon metabolism in health and disease. *Cell Metab.* 2017;25:27–42. [PubMed: 27641100]
38. Labuschagne CF, van den Broek NJF, Mackay GM, Vousden KH, Maddocks ODK. Serine, but not glycine, supports one-carbon metabolism and proliferation of cancer cells. *Cell Rep.* 2014;7:1248–58. [PubMed: 24813884]
39. Ducker GS, Ghergurovich JM, Mainolfi N, Suri V, Jeong SK, Hsin-Jung Li S, et al. Human SHMT inhibitors reveal defective glycine import as a targetable metabolic vulnerability of diffuse large B-cell lymphoma. *Proc Natl Acad Sci.* 2017;114:11404–11409. [PubMed: 29073064]
40. Celià-Terrassa T, Kang Y. Distinctive properties of metastasis-initiating cells. *Genes Dev.* 2016;30:892–908. [PubMed: 27083997]
41. Fan J, Teng X, Liu L, Mattaini KR, Looper RE, Vander Heiden MG, et al. Human phosphoglycerate dehydrogenase produces the oncometabolite D –2-hydroxyglutarate. *ACS Chem Biol.* 2015;10:510–6. [PubMed: 25406093]
42. Yang M, Vousden KH. Serine and one-carbon metabolism in cancer. *Nat Rev Cancer.* 2016;16:650–662. [PubMed: 27634448]
43. Bernhardt S, Bayerlová M, Vetter M, Wachter A, Mitra D, Hanf V, et al. Proteomic profiling of breast cancer metabolism identifies SHMT2 and ASCT2 as prognostic factors. *Breast Cancer Res.* 2017;19:112. [PubMed: 29020998]
44. Poli V, Fagnocchi L, Fasciani A, Cherubini A, Mazzoleni S, Ferrillo S, et al. MYC-driven epigenetic reprogramming favors the onset of tumorigenesis by inducing a stem cell-like state. *Nat Commun.* 2018;9:1024. [PubMed: 29523784]
45. Lee HY, Cha J, Kim SK, Park JH, Song KH, Kim P, et al. c-MYC drives breast cancer metastasis to the brain, but promotes synthetic lethality with TRAIL. *Mol Cancer Res.* 2019;17:544–54. [PubMed: 30266755]
46. Nigdelioglu R, Hamanaka RB, Meliton AY, O’Leary E, Witt LJ, Cho T, et al. Transforming Growth Factor (TGF)- β Promotes *de Novo* Serine Synthesis for Collagen Production. *J Biol Chem.* 2016;291:27239–51. [PubMed: 27836973]
47. Yin JJ, Selander K, Chirgwin JM, Dallas M, Grubbs BG, Wieser R, et al. TGF- β signaling blockade inhibits PTHrP secretion by breast cancer cells and bone metastases development. *J Clin Invest.* 1999;103:197–206. [PubMed: 9916131]
48. Fournier PGJ, Juárez P, Jiang G, Clines GA, Niewolna M, Kim HS, et al. The TGF- β Signaling Regulator PMEPA1 Suppresses Prostate Cancer Metastases to Bone. *Cancer Cell.* 2015;27:809–21. [PubMed: 25982816]

Implications:

This study identifies mitochondrial serine and 1C unit metabolism as an important pathway during the progression of a subset of human breast cancers.

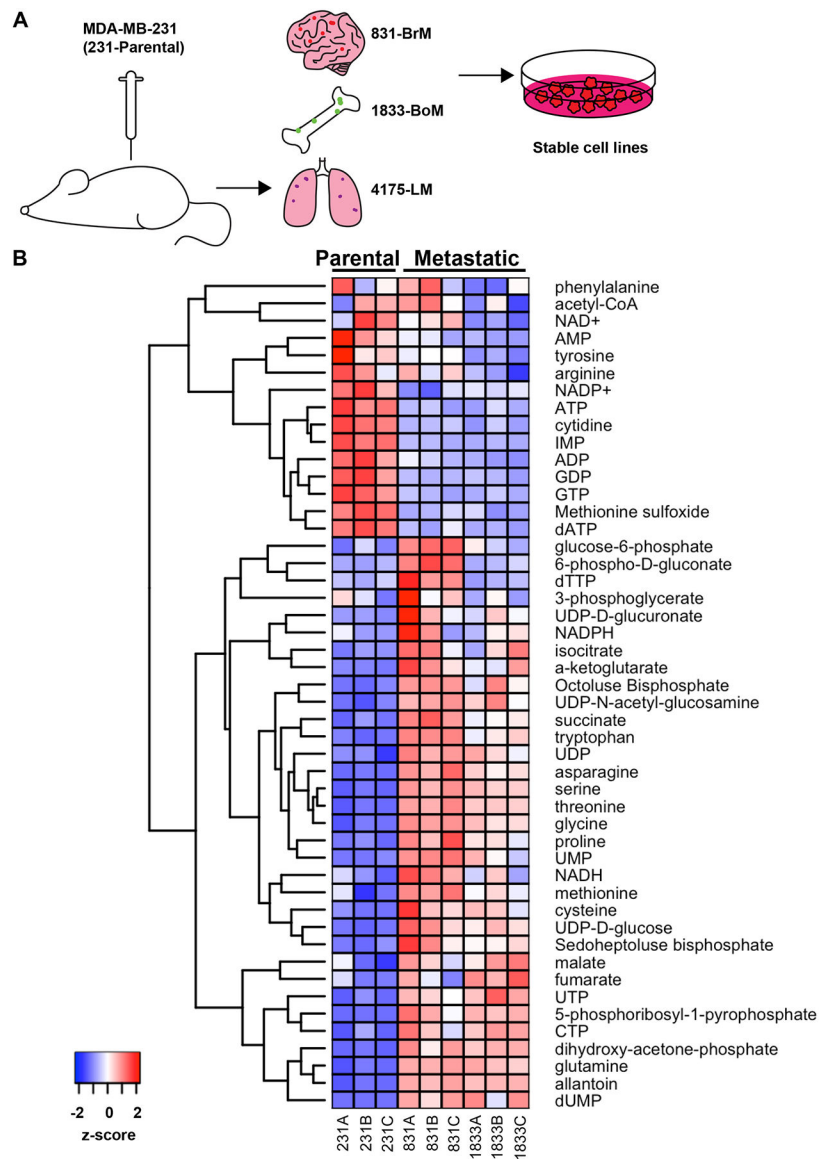


Figure 1. Metastatic breast cancer subclones display an altered metabolic profile. **(A)** Schematic of targeted metabolomics workflow. Brain (831-BrM), bone (1833-BoM), and lung (4175-LM) metastatic subclones from tissue-tropic subpopulations were generated following IV injection of a parental population of MDA-MB-231 (231-Parental) cells into the tail vein or heart. Stable cell lines were passaged in culture prior to metabolite extraction for LC-MS/MS. **(B)** LC-MS profile of the 231-Parental, 831-BrM, and 1833-BoM cell lines. Cell lines were plated in biological triplicates prior to metabolite extraction. Signals were normalized to the mean signal of each metabolite across all samples, log₂ transformed, and clustered.

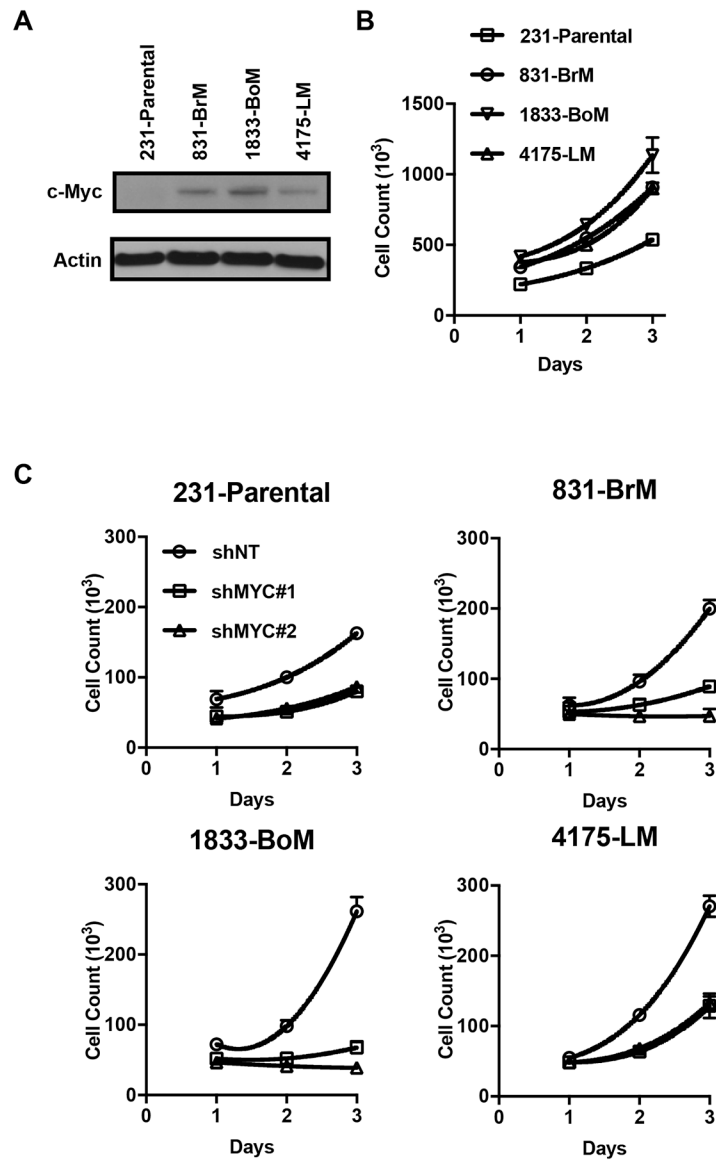


Figure 2. c-Myc drives proliferation in metastatic breast cancer cell subclones. **(A)** IB for c-Myc from whole-cell extracts of parental and metastatic subclones. **(B)** Proliferation of parental cells and metastatic subclones over 3 days (mean \pm SD, n = 3). **(C)** 3 day proliferation of 231-Parental, 831-BrM, 1833-BoM, and 4175-LM cells expressing either a nontargeting (shNT) or c-Myc targeting (shMyc) vectors. (mean \pm SD, n = 3).

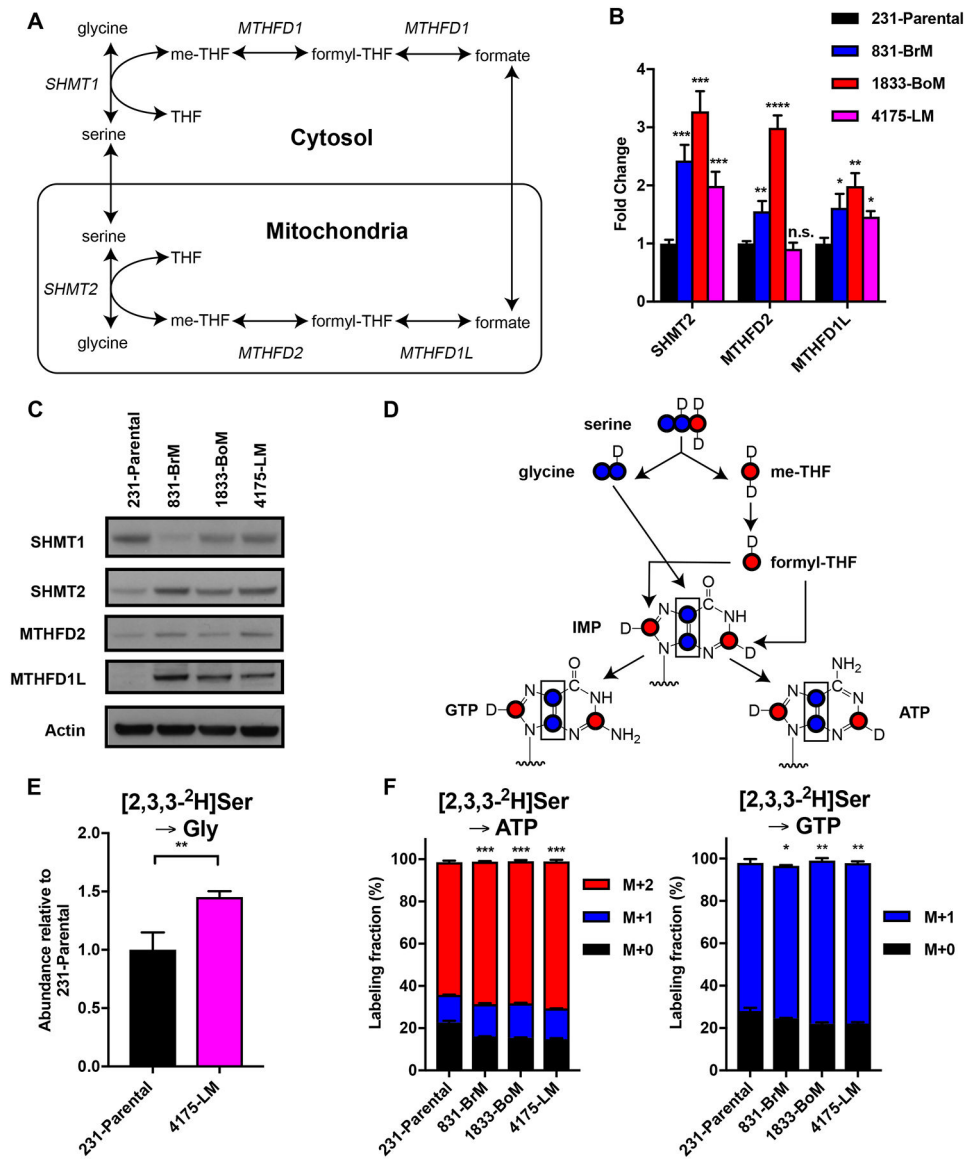


Figure 3. The mitochondrial serine and one-carbon unit pathway is upregulated in metastatic breast cancer subclones. **(A)** Schematic of the cytosolic and mitochondrial serine and one-carbon unit pathway. **(B)** qPCR for serine and one-carbon unit pathway genes (mean \pm SD, $n = 3$, $*P < 0.05$ $**P < 0.01$ $***P < 0.001$ $****P < 0.0001$ by two-tailed Student's *t* test, compared to expression in parental cells). **(C)** IB for serine and one-carbon unit pathway enzymes from whole-cell extracts of parental cells and metastatic subclones. **(D)** Schematic diagram of incorporation of ^2H (D) from [2,3,3- ^2H]serine onto glycine, one-carbon units, and purines. **(E)** SHMT flux estimated by relative abundance of labeled glycine from serine (mean \pm SD, $n = 3$, $**P < 0.01$ by two-tailed Student's *t* test). **(F)** Fractional labeling of [2,3,3- ^2H]serine onto GTP and ATP (mean \pm SD, $n = 3$, $*P < 0.05$ $**P < 0.01$ $***P < 0.001$ by two-tailed Student's *t* test).

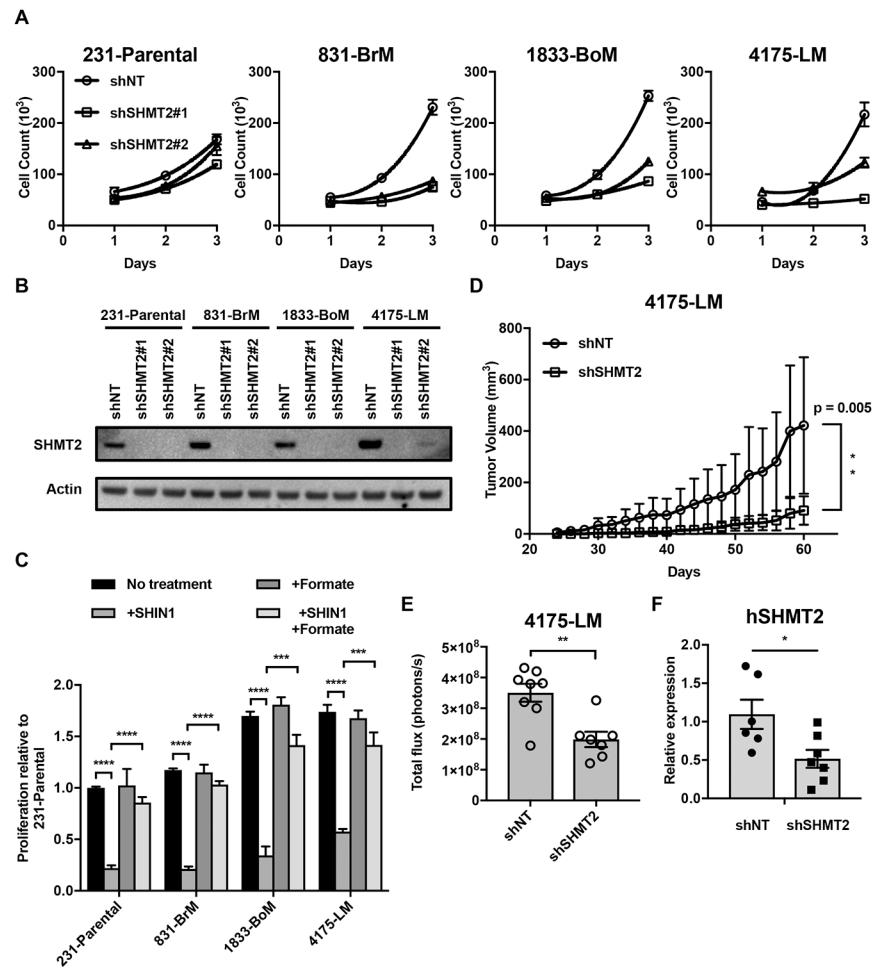


Figure 4. Metastatic subclones are particularly sensitive to SHMT2 inhibition. **(A)** 3 day proliferation of 231-Parental, 831-BrM, 1833-BoM, and 4175-LM cells expressing either a nontargeting (shNT) or SHMT2 targeting (shSHMT2) vectors. Relative proliferation was calculated relative to average proliferation of shNT cells (mean \pm SD, $n = 3$). **(B)** IB for SHMT2 in parental and metastatic subclones. **(C)** 3 day proliferation of parental and metastatic cells with 2 μM SHIN1, in RPMI with or without 2 mM formate and dialyzed FBS (mean \pm SD, $n = 3$, *** $P < 0.001$ **** $P < 0.0001$ by two-tailed Student's t test). Counts were normalized to the proliferation of 231-Parental cells in media without SHIN1 and formate treatment. **(D)** Growth of 4175-LM shNT and shSHMT2 tumors in the mammary fat pad of nude mice (mean \pm SEM, $n = 8$, ** $P < 0.01$ by two-tailed Student's t test). **(E)** Quantification of luminescence signal in the lungs of mice 3 weeks post injection of either 4175-LM shNT or shSHMT2 cells (mean \pm SEM, ** $P < 0.01$ by two-tailed Student's t test, shNT; $n = 8$ shSHMT2; $n = 7$). **(F)** qPCR analysis of hGAPDH expression in the lungs of mice 4 weeks post injection of either 4175-LM shNT or shSHMT2 cells (mean \pm SEM, * $P < 0.05$ by two-tailed Student's t test, shNT; $n = 6$ shSHMT2; $n = 7$).

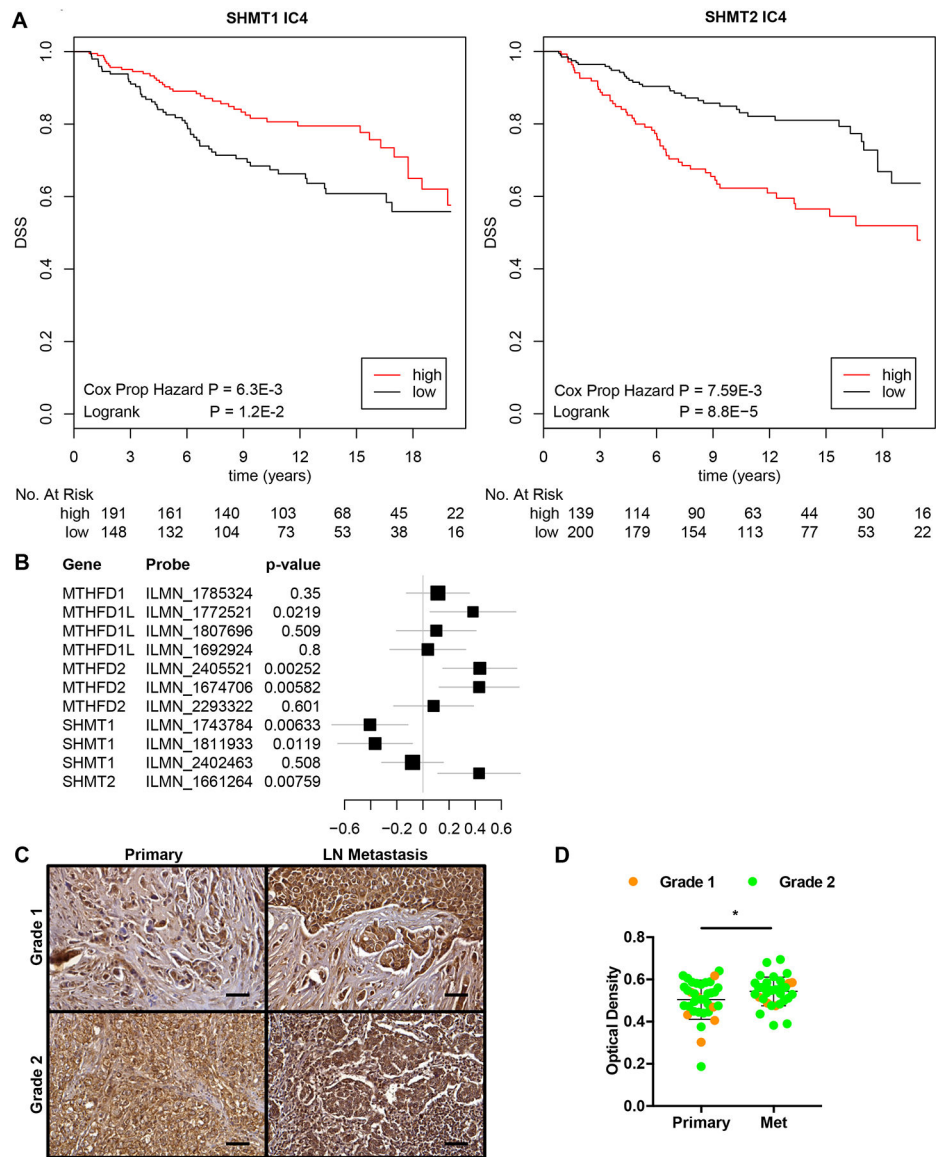


Figure 5. Mitochondrial serine and one-carbon unit pathway enzyme expression correlates with poor survival in human breast cancer. **(A)** Kaplan-Meier plot for SHMT1 (left) and SHMT2 (right) expression associated with disease-specific survival (DSS) in the human IC4 patient subgroup (METABRIC). **(B)** Forest plot for the hazard of individual 1C unit pathway genes adjusted for covariates (age, grade, size, number of lymph nodes, ER, PR and Her2 status) in the IC4 subgroup (n=343). **(C)** Representative SHMT2 staining (at 40x) of human breast invasive ductal carcinoma and matched metastatic carcinoma tissue samples (LN = lymph node). **(D)** Quantification of SHMT2 intensity by IHC in metastatic lesions compared to primary tumors (mean \pm SD, n = 33 per group, *P < 0.05 by two-tailed Student's t test).

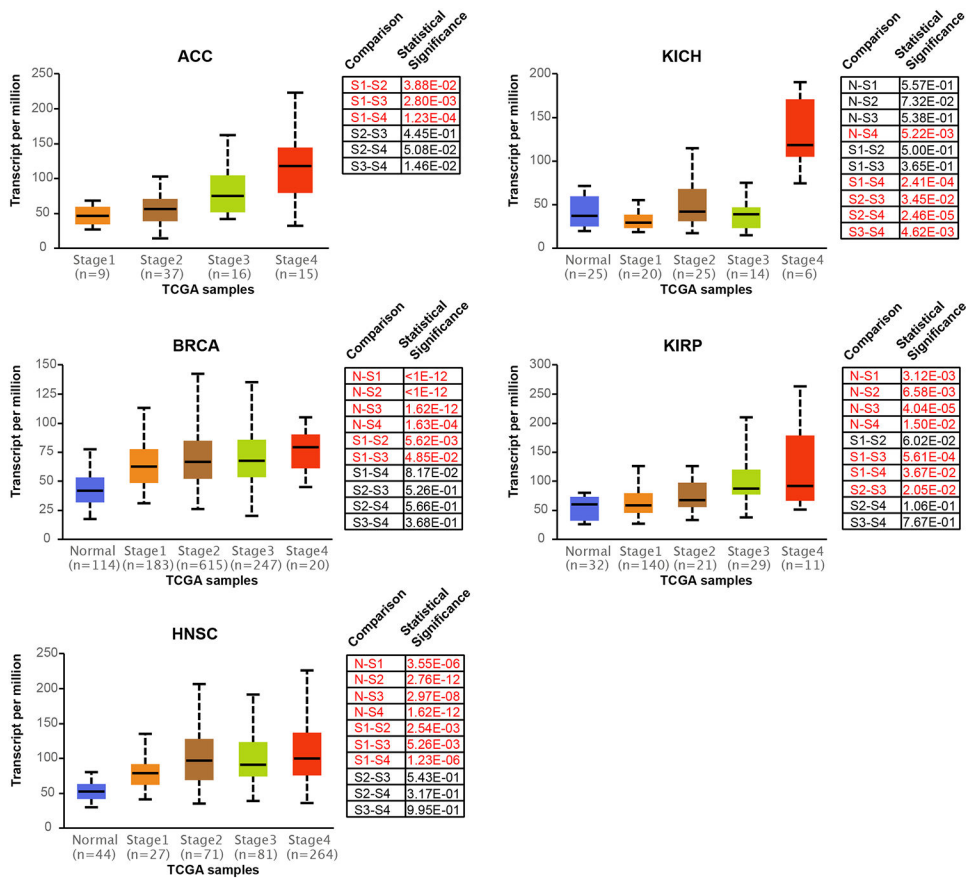


Figure 6. SHMT2 expression increases with stage in various cancers.

Box plots depicting the average expression level (transcripts per million) of SHMT2 in normal tissue (N) and as a function of cancer stage (stage 1 = S1; stage 2 = S2; stage 3 = S4; stage 4 = S4). Statistically significant differences between pairwise comparisons are highlighted in red. Abbreviations for cancer types are explained as follows: ACC (adrenocortical carcinoma), BRCA (breast invasive carcinoma), HNSCC (head and neck squamous cell carcinoma), KICH (kidney chromophobe carcinoma), KIRP (kidney renal papillary cell carcinoma).